



In Vitro and *In Vivo* Studies of the Trypanocidal Effect of Novel Quinolines

A. S. G. Nefertiti,^a M. M. Batista,^a P. B. Da Silva,^a D. G. J. Batista,^a C. F. Da Silva,^a R. B. Peres,^a  E. C. Torres-Santos,^b E. F. Cunha-Junior,^b E. Holt,^c D. W. Boykin,^c R. Brun,^{d,e} T. Wenzler,^{d,e*} M. N. C. Soeiro^a

^aLaboratório de Biologia Celular, Instituto Oswaldo Cruz, Fundação Oswaldo Cruz, Rio de Janeiro, Rio de Janeiro, Brazil

^bLaboratório de Bioquímica de Tripanossomatídeos, Instituto Oswaldo Cruz, Fundação Oswaldo Cruz, Rio de Janeiro, Rio de Janeiro, Brazil

^cDepartment of Chemistry, Georgia State University, Atlanta, Georgia, USA

^dSwiss Tropical and Public Health Institute, Basel, Switzerland

^eUniversity of Basel, Basel, Switzerland

ABSTRACT Therapies for human African trypanosomiasis and Chagas disease, caused by *Trypanosoma brucei* and *Trypanosoma cruzi*, respectively, are limited, providing minimal therapeutic options for the millions of individuals living in very poor communities. Here the effects of 10 novel quinolines are evaluated *in silico* and by phenotypic studies using *in vitro* and *in vivo* models. Absorption, distribution, metabolism, excretion, and toxicity (ADMET) properties revealed that most molecules did not infringe on Lipinski's rules, which is a prediction of good oral absorption. These quinolines showed high probabilities of Caco2 permeability and human intestinal absorption and low probabilities of mutagenicity and of hERG1 inhibition. *In vitro* screens against bloodstream forms of *T. cruzi* demonstrated that all quinolines were more active than the reference drug (benznidazole [Bz]), except for DB2171 and DB2192, with five (DB2187, DB2131, DB2186, DB2191, and DB2217) displaying 50% effective concentrations (EC₅₀s) of <3 μM (4-fold lower than that of Bz). Nine quinolines were more effective than Bz (2.7 μM) against amastigotes, showing EC₅₀s ranging from 0.6 to 0.1 μM. All quinolines were also highly active *in vitro* against African trypanosomes, showing EC₅₀s of ≤0.25 μM. The most potent and highly selective candidates for each parasite species were tested in *in vivo* models. Results for DB2186 were promising in mice with *T. cruzi* and *T. brucei* infections, reaching a 70% reduction of the parasitemia load for *T. cruzi*, and it cured 2 out of 4 mice infected with *T. brucei*. DB2217 was also active *in vivo* and cured all 4 mice (100% cure rate) with *T. brucei* infection.

KEYWORDS *Trypanosoma cruzi*, *Trypanosoma brucei*, experimental chemotherapy, quinolines, *in vitro*, *in vivo*, *in silico*

Currently, more than 1 billion people live in poverty, without access to basic sanitation, favoring the emergence and development of various diseases. The WHO grouped 20 pathologies caused by viruses, fungi, bacteria, protozoans, and helminths, named neglected tropical diseases, that have a severe impact in on public health programs of developing countries but present low interest and investments for the development of early diagnostic tools and safer/potent therapies by most pharmaceutical companies (<https://www.dndi.org/>) (1, 2).

Human African trypanosomiasis (HAT), or sleeping sickness, is a lethal disease in sub-Saharan Africa caused by two subspecies of *Trypanosoma brucei*: *Trypanosoma brucei gambiense* is endemic in western and central Africa, and *Trypanosoma brucei rhodesiense* is most prevalent in eastern and southern Africa (3). Both parasite subspe-

Received 15 September 2017 Returned for modification 29 October 2017 Accepted 20 November 2017

Accepted manuscript posted online 4 December 2017

Citation Nefertiti ASG, Batista MM, Da Silva PB, Batista DGJ, Da Silva CF, Peres RB, Torres-Santos EC, Cunha-Junior EF, Holt E, Boykin DW, Brun R, Wenzler T, Soeiro MNC. 2018. *In vitro* and *in vivo* studies of the trypanocidal effect of novel quinolines. Antimicrob Agents Chemother 62: e01936-17. <https://doi.org/10.1128/AAC.01936-17>.

Copyright © 2018 American Society for Microbiology. All Rights Reserved.

Address correspondence to M. N. C. Soeiro, soeiro@ioc.fiocruz.br.

* Present address: T. Wenzler, Institute of Cell Biology, University of Bern, Bern, Switzerland.

cies are transmitted by the bite of an infected tsetse fly (genus *Glossina*). Clinical presentations vary according to the subspecies and the disease stage. The symptoms of the hemolymphatic stage are mostly nonspecific and include fever, headache, and swelling of the lymph nodes. In the second, meningoencephalitic stage, the trypomastigotes infect the central nervous system in addition to the blood and lymph system. Neurological symptoms such as mental confusion and emotional lability as well as convulsions and alteration of the circadian rhythm, a characteristic giving the disease its name, accompany the second stage. Sleeping sickness is fatal, if left untreated (3).

Chagas disease (CD), also a neglected tropical disease, is endemic in 21 countries in Latin America, constituting a continuing serious public health problem and presenting a chronic progressive pathology that affects more than 6 million to 8 million people worldwide (<https://www.dndi.org/>). CD is caused by the protozoan *Trypanosoma cruzi*, and its transmission occurs primarily via bug triatomine vectors and may also include other routes such as blood transfusion, congenital transmission (both of which are declining due to public health measures adopted by countries where the disease is endemic), laboratory accidents, and ingestion of food and drinks contaminated with the feces of and/or entire triatomines containing infective forms of the parasite (4). Current treatment of CD is based on two nitroheterocyclic drugs, nifurtimox (Nif) and the 2-nitroimidazole benznidazole (Bz), introduced into clinical therapy over 5 decades ago (5). Recent clinical trials (6, 7) performed on chronically infected patients to evaluate the azole inhibitors of CYP51 (prodrug of ravuconazole and posaconazole) and a nitroderivative (fexinidazole) showed high rates of therapeutic failure despite their excellent activity *in vitro* and *in vivo* using experimental models (mouse and canine models), arguing for the generation of more predictive *in vitro* and *in vivo* data (5, 8, 9).

For HAT, a total of five drugs are available. However, treatment recommendations fall back to one option for each subspecies and disease stage. Pentamidine (*T. b. gambiense*) and suramin (*T. b. rhodesiense*) are used as first-line treatments for first-stage disease, and melarsoprol (*T. b. rhodesiense*) and a combination of eflornithine and nifurtimox (*T. b. gambiense*) are used for second-stage disease (1). The main general limitations of the current therapies for both HAT and CD include considerable adverse effects, high costs, the requirement for long periods of exposure, the occurrence of natural and acquired resistant parasites, and treatment failures, especially in the later pathological stages (9). These findings underscore the urgent need to search for new trypanocidal agents with characteristics for each target product profile (for CD and HAT) (<https://www.dndi.org/>) (4, 10). In this context, many compounds have been tested *in vitro* and *in vivo*, but until now, only a few candidates have been found (5, 11–13).

The present work with quinolines is based on a high-throughput phenotypic screening of a library of 700,000 compounds by the Genomics Institute of the Novartis Research Foundation. It yielded over a hundred different scaffolds that were nontoxic to human cells and were active (3.6 μM or lower) against *T. brucei* (14). One of the initial hits, 2-(2-benzamido)ethyl-4-phenylthiazole, has been extensively explored, and a number of compounds that were highly active against *T. brucei in vitro* were discovered (15). However, these compounds were only moderately effective in the STIB900 mouse model of *T. b. rhodesiense* infections, which was attributed, at least in part, to poor metabolic stability (15). We undertook an exploration of *N*-(2-phenylquinolin-7-yl)benzamides and related compounds, which retain similar geometric relationships between the amide unit and the thiazole nitrogen atom hypothesized to be important for activity. In this quinoline system, the "ethylamine link" of the original thiazole hit is incorporated into the quinoline ring and may improve metabolic stability. While our study was in progress, excellent *in vivo* results against both early- and late-stage *T. brucei* infections in mice for a benzothiazole analogue of the initial hit were reported by that same group (15).

Thus, in this work, we investigate the phenotypic activities of 10 novel quinolines through whole-cell-based assays *in vitro* by assaying different parasite forms (trypomastigotes and amastigotes) and strains (discrete typing unit [DTU] II and VI) of *T. cruzi*

in addition to exploring their biological activities against bloodstream forms of *T. b. rhodesiense* *in vitro*. Furthermore, the toxicity profiles of these quinolines were studied by using different mammalian cells and by their predictive pharmacological properties evaluated by pKCSM. Finally, the most promising compounds were moved to animal models of *T. b. rhodesiense* and *T. cruzi* infections, with the aim to contribute to the identification of novel therapeutic options for these severe neglected pathologies.

RESULTS

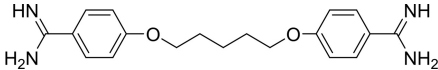
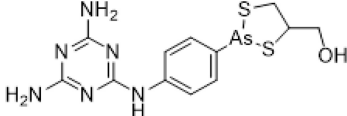
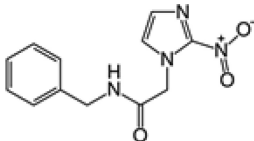
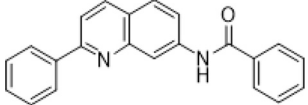
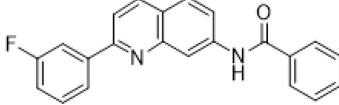
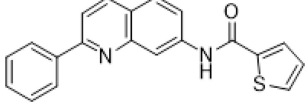
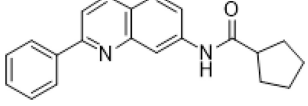
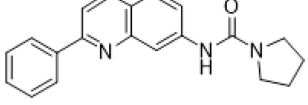
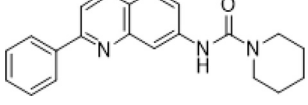
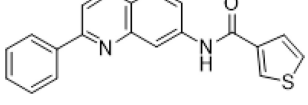
A phenotypic *in vitro* study using the 10 quinoline derivatives (Table 1) was performed on *T. cruzi* and *T. brucei* parasites. Considering that all active drug candidates for *T. cruzi* must also be assessed against the relevant intracellular forms (16), the initial step consisted of analyses of intracellular forms (Tulahuen strain transfected with β -galactosidase [DTU VI] and Y strain [DTU II]). Our findings for the Tulahuen strain showed that all quinolines were more potent than Bz when infected L929 cells were incubated for 96 h at 37°C, with 50% effective concentrations (EC_{50} s) ranging from 0.1 μ M up to 2.05 μ M and selectivity indices (SI) ranging from 48 up to 960 (Table 1). By screening against intracellular forms of the Y strain lodged inside cardiac cells (CC), the trypanocidal efficacy of quinolines was confirmed, as DB2187 exhibited a low EC_{50} ($1.03 \pm 0.3 \mu$ M) (data not shown).

Following 24 h of incubation with trypomastigote forms of *T. cruzi* (Y strain [DTU II]), except for DB2171 and DB2192, all quinolines presented higher trypanocidal activity than that of Bz, exhibiting EC_{50} s of $\leq 8 \mu$ M (Table 1). Among these quinolines, DB2187 and its analogue DB2186 were the most effective (EC_{50} of $\leq 0.8 \mu$ M), being about 12-fold more potent than the reference drug. All molecules also showed high trypanocidal activity against *T. brucei* bloodstream forms, with EC_{50} s ranging from 0.016 to 0.239 μ M, and strong selectivity for this parasite, with selectivity indices ranging from 88 to 5,455 (Table 1). The cytotoxicity data for the studied quinolines using colorimetric assays with PrestoBlue (cardiac cells) and alamarBlue (L929 cultures) showed that all molecules were tolerated, with no detectable toxicity at concentrations of up to 96 μ M after 24 to 96 h of incubation (data not shown). The lack of mammalian host toxicity was confirmed when DB2104, DB2131, DB2161, DB2171, and DB2191 were tested (up to 48 h) using higher concentrations on cardiac cells (up to 400 μ M) (data not shown). Cytotoxicity against L6 cells was also low and varied from 15 μ M (DB2217) to $>270 \mu$ M (DB2187). Fifty percent lethal concentrations (LC_{50} s) of each compound on L6 cells can be deduced from the SI of *T. b. rhodesiense* (Table 1).

For both parasite species (*T. brucei* and *T. cruzi*), DB2186 was the most potent molecule from this series, without inhibiting mammalian cells. Absorption, distribution, metabolism, excretion, and toxicity (ADMET) properties of quinolines predicted by using the pKCSM tool revealed that DB2186, DB2187, DB2192, and DB2217 did not infringe on Lipinski's rule of five, which is a prediction of good oral absorption (Table 2). The quinolines showed a good probability of permeability on Caco2 cells, with values above the adopted threshold of 0.9; probabilities of human intestinal absorption of $>89\%$, with an even better oral absorption profile than that of Bz; and a positive prediction to be metabolized by CYP3A4 (Table 3). These quinolines have a low probability of mutagenicity and no prediction to inhibit hERG1, although they all show the possibility of inhibiting hERG2 and a hepatotoxicity profile similar to that of Bz (Table 4). Evaluation of hepatic markers in biochemical analyses *in vivo* using mouse models of acute toxicity demonstrated no alterations of the plasma levels of alanine aminotransferase (ALT) (except for DB2192), aspartate aminotransferase (AST), urea, and creatine kinase (CK) in addition to no major clinical signs (except for losses of animal weight) when mice were given up to 200 mg/kg of body weight of DB2187 and its derivatives DB2186, DB2191, and DB2192 and monitored up to 48 h (data not shown). Next, based on the excellent phenotypic findings and lack of preliminary acute toxicity indications, DB2187 and derivatives were moved to *in vivo* antiparasitic analyses using mouse models.

Male mice inoculated with 10^4 bloodstream forms (*T. cruzi* Y strain) and treated

TABLE 1 Antitrypanosomal activities of novel quinolines against bloodstream trypomastigotes of *T. brucei* and intracellular and bloodstream forms of *T. cruzi* and corresponding selective indices^a

Chemical structure	Compound	Mean EC ₅₀ (μM) ± SD (SI value)		
		<i>T. b. rhodesiense</i> BT forms	<i>T. cruzi</i>	
			BT forms	Intracellular forms
	Pentamidine	0.003 (11.4368)	NT	NT
	Melarsoprol	0.004 (1.275)	NT	NT
	Benznidazole	NT	9.6 ± 1.4 (>104)	2.7 ± 1 (370)
	DB2104	0.213 (971)	6.1 ± 2.8** (>66)	0.54 ± 0.2 (>178)
	DB2131	0.204 (229)	2.5 ± 1.1** (>160)	0.6 ± 0.3 (>160)
	DB2161	0.076 (1.164)	8 ± 2.9 (>50)	0.5 ± 0.038 (>192)
	DB2171	0.239 (983)	15 ± 8 (>27)	2.05 ± 0.6 (>47)
	DB2186	0.016 (1.761)	0.78 ± 0.46** (>123)	0.15 ± 0.01 (>640)
	DB2187	0.050 (>5.455)	0.8 ± 0.2** (>137)	0.36 ± 0.12 (>233)
	DB2191	0.057 (647)	2.6 ± 0.64** (>154)	0.1 ± 0 (>960)

(Continued on next page)

TABLE 1 (Continued)

Chemical structure	Compound	Mean EC ₅₀ (μM) ± SD (SI value)		
		<i>T. b. rhodesiense</i> BT forms	<i>T. cruzi</i> BT forms	Intracellular forms
	DB2192	0.045 (3.828)	24 ± 5.8 (>4)	0.1 ± 0.001 (>960)
	DB2212	0.123 (>2.118)	7.2 ± 3.2 (>12)	0.3 ± 0.039 (>320)
	DB2217	0.170 (88)	2.7 ± 1.2** (>36)	0.41 ± 0.27 (>234)

α**, *P* < 0.05 as determined by ANOVA of the studied compound and Bz; SI, selectivity index; NT, not tested.

(intraperitoneally [i.p.]) at 5 and 8 days postinfection (dpi) using nontoxic concentrations of DB2187 gave a maximum reduction of parasitemia of 38% at the peak (8 dpi) in comparison to the vehicle group but failed to protect against mortality induced by parasite infection (Table 5). The administration of nontoxic concentrations of DB2186, DB2191, and DB2192 at 25 mg/kg/day for five consecutive days in *T. cruzi*-infected male and female mice showed that DB2186 was the most active compound, reaching 25 and 70% reductions of the blood parasitemia loads, respectively, when 25 mg/kg was given for five consecutive days, while Bz completely suppressed parasitism (Table 5). Regarding the effects on mortality induced by experimental *T. cruzi* infection, infected female and male mice treated with the vehicle only displayed 50 and 17% survival rates, respectively, whereas all the Bz-treated animals were alive. The tested quinolines were not able to provide significant protection against mortality (Table 5).

The quinolines were also evaluated for their antitrypanosomal efficacy in *T. b. rhodesiense*-infected mice. In the preliminary experiment, the compounds were tested on small groups of 2 mice treated at 40 mg/kg/day i.p. for three consecutive days. Six compounds showed activity on the level of a strong reduction of parasitemia (>98%) in at least one of the two mice and were well tolerated at the tested dosage (Table 6). These compounds were further tested in 4 infected mice at a higher dosage of 50 mg/kg/day i.p. for four consecutive days. DB2186 and DB2217 were the best molecules and cured 2 of 4 infected mice and all 4 infected mice, respectively (Table 6).

TABLE 2 Physicochemical parameters and Lipinski's rule of five^a

Compound	Water solubility (mg/liter)	No. of donors	No. of acceptors	LogP	MW
DB2104	2.394	2	4	5.154	324.383
DB2131	1.041	2	4	5.293	342.373
DB2161	1.416	3	4	5.215	330.412
DB2171	2.775	2	4	5.030	316.404
DB2186	3.887	2	4	4.529	317.392
DB2187	-5.9	1	2	4.9	333.419
DB2191	1.416	3	4	5.215	330.412
DB2192	5.356	2	4	4.305	315.376
DB2212	0.934	2	4	5.309	345.446
DB2217	2.587	2	4	4.695	329.403
Bz	376.248	1	5	0.11	260.253

^aMW, molecular weight; LogP, partition coefficient.

TABLE 3 *In silico* ADME^a

Parameter	Value for compound										
	DB2104	DB2131	DB2161	DB2171	DB2186	DB2187	DB2191	DB2192	DB2212	DB2217	Bz
Absorption											
Caco2 cell permeability (log cm/s)	1.491	1.163	1.773	1.765	1.373	1.21	1.773	1.361	1.158	1.384	0.479
Intestinal absorption (human) (%)	94.747	89.969	89.46	90.659	90.877	91.515	89.46	91.353	90.1	90.964	68.885
Skin permeability (logKp)	-2.763	-3.167	-3.118	-3.092	-3.214	-3.012	-3.118	-3.238	-3.198	-3.23	-2.893
Distribution											
V _{ss} (human) (liters/kg)	0.345	5.521	5.140	6.124	4.721	-0.115	5.140	4.624	5.508	4.989	0.787
Fraction unbound (human)	0	0.278	0.292	0.3	0.321	0.064	0.292	0.331	0.275	0.307	0.503
BBB permeability	0.264	0.265	0.241	0.254	0.201	0.269	0.241	0.2	0.227	0.213	-0.619
CNS permeability	-1.013	-2.778	-2.687	-2.687	-2.691	-1.639	-2.687	-2.691	-2.782	-2.737	-2.995
Metabolism											
CYP2D6 substrate	No	No	No	No	No	No	No	No	No	No	No
CYP3A4 substrate	Yes	Yes	Yes	Yes	Yes	Yes	Yes	Yes	Yes	Yes	No
CYP1A2 inhibitor	Yes	Yes	Yes	Yes	Yes	Yes	Yes	Yes	Yes	Yes	No
CYP2C19 inhibitor	Yes	Yes	Yes	Yes	Yes	Yes	Yes	Yes	Yes	Yes	No
CYP2C9 inhibitor	Yes	No	No	No	No	No	No	No	No	No	No
CYP2D6 inhibitor	No	No	No	No	No	No	No	No	No	No	No
CYP3A4 inhibitor	No	No	No	No	No	No	No	No	No	No	No
Excretion											
Total clearance (ml/min/kg)	3.793	6.998	12.023	10.162	8.433	0.545	12.023	6.714	6.823	6.368	4.217

^aV_{ss}, volume of distribution at steady state; BBB, blood-brain barrier; CNS, central nervous system; logKp, skin permeability constant (cm/h).

DISCUSSION

Most drug development programs for neglected diseases are time-consuming (often more than 10 years) and highly expensive (more than \$1 billion) and get only limited attention by the pharmaceutical industry. Until now, no vaccine has been available for Chagas disease and for HAT, and the current therapies available have strong liabilities; thus, novel therapeutic options are urgently needed. Drug discovery and development strategies include phenotypic screening of synthetic and natural molecules, assessment of combination therapies, repurposing of medicines, and drug development toward selective parasite targets (11, 17, 18). Our goal was to investigate the biological effects *in vitro* and *in vivo* of the 10 novel quinoline derivatives (Table 1) on *T. cruzi* and *T. brucei* infections. We conducted different analyses that included computational and cell-based screening as well as mouse models of trypanosome infections. As reported previously, *in silico* analyses have the advantages of low cost, fast processing, and the fact that compounds can be evaluated without synthesizing them, allowing large libraries to be explored (22). However, computational screens

TABLE 4 *In silico* toxicity^a

Parameter	Value for compound										
	DB2104	DB2131	DB2161	DB2171	DB2186	DB2187	DB2191	DB2192	DB2212	DB2217	Bz
AMES toxicity	No	No	No	No	No	No	No	No	No	No	Yes
Max tolerated dose (human) (mol/kg)	17.418	1.393	1.758	1.807	1.758	0.784	1.758	1.766	1.330	1.535	9.638
hERG1 inhibitor I	No	No	No	No	No	No	No	No	No	No	No
hERG2 inhibitor	Yes	Yes	Yes	Yes	Yes	Yes	Yes	Yes	Yes	Yes	No
Oral rat acute toxicity (LD ₅₀) (mol kg ⁻¹)	2.535	2.906	2.924	2.719	2.817	2.856	2.924	2.783	2.885	2.819	2.454
Oral rat chronic toxicity (LOAEL) (mg/kg of body wt/day)	289.068	46.345	61.094	80.168	47.973	1.878	61.094	43.451	46.345	42.756	44.566
Hepatotoxicity	Yes	Yes	Yes	Yes	Yes	Yes	Yes	Yes	Yes	Yes	Yes
Skin sensitization	No	No	No	No	No	No	No	No	No	No	No
<i>Tetrahymena pyriformis</i> toxicity (pIGC ₅₀ [μg/liter])	5.929	29.923	33.884	31.405	31.842	1.256	33.884	31.333	28.642	30.479	16.866
Minnnow toxicity (LC ₅₀ [mM])	0.586	4.732	3.365	4.325	6.039	0.739	3.365	7.244	3.524	5.534	44.566

^aLD₅₀, 50% lethal dose; LOAEL, lowest observed adverse effect level; pIGC₅₀, negative logarithm of the concentration required to inhibit 50% growth (in log μg/liter).

TABLE 5 Antitrypanosomal activities of quinolines in mouse models of *T. cruzi* infection (Y strain) using 25 mg/kg (i.p.) for five consecutive days starting at parasitemia onset (5 dpi)

Compound	Mouse gender	% parasite variation at parasitemia peak (8 dpi)	% cumulative mortality at 30 days posttherapy
Benznidazole ^a	Female	100	0
	Male	100	0
Vehicle	Female	0	50
	Male	0	83
DB2187 ^b	Male	−38	100
DB2186	Female	−25	75
	Male	−70	50
DB2191	Female	−9	50
	Male	−27	100
DB2192	Female	+74	33
	Male	+28	100

^aBenznidazole was tested at 100 mg/kg p.o.^bDB2187 was tested at 20 mg/kg i.p. at 5 and 8 dpi.

often fail to simulate the full complexity of biological systems and need to be complemented with experimental studies (19). Here, the antiparasitic activities of the novel quinolines were explored, considering different aspects of the drug discovery cascade performed in *in silico*, *in vitro* (whole-cell-based), and *in vivo* (the most biologically realistic) assays, according to current strategies for hit and lead identification for novel anti-*T. cruzi* and anti-*T. brucei* drugs. Our findings demonstrated the promising *in vitro* activities of these compounds against both bloodstream trypomastigotes (*T. cruzi* and *T. brucei*) and intracellular forms (*T. cruzi*) of these parasites, with most molecules exhibiting greater potency than the reference drug for Chagas disease (Bz). The quinolines also have the potential to be developed for *T. brucei*, although they were less potent than the highly toxic compound melarsoprol or the *T. b. gambiense* first-stage drug pentamidine. The quinoline DB2186 was very active against both trypanosome species regardless of the parasite form, displaying quite high selectivity indices that were even superior to those reported previously for novel hits for CD and HAT (11, 12, 20). Regarding *T. cruzi* screens, the quinolines were active against parasite strains from different DTUs (DTUs II and VI for the Y and Tulahuen strains, respectively), furthermore showing low toxicity toward mammalian host cells, including primary cultures of cardiac cells that provide, in a more sensitive manner, the potential for *in vivo* cardiotoxicity. These are very critical data since the heart represents an important target for *T. cruzi* infection and inflammation (21). In fact, plasma biochemical analyses of quinoline-treated mice confirmed the low-cardiotoxicity profile determined by CK measurements. Thus, *in vitro* whole-cell-based screening associated with theoretical analyses of the ADMET properties and mouse models of acute toxicity were used to select potential drug candidates to proceed to *in vivo* efficacy evaluations (22). The *in silico* properties of the novel quinolines were evaluated by using the pKCSM tool, and the overall findings predicted good oral absorption, a high probability of permeability in Caco2 cells, good human intestinal absorption, and low probabilities of mutagenicity and inhibition of hERG1. The preliminary acute murine toxicity assays failed to demonstrate increased levels of hepatic lesion markers such as ALT and AST, except for DB2192 (statistically significant enhancement of ALT levels, indicative of hepatic damage). To evaluate efficacy *in vivo* against *T. cruzi* infection, both female and male mouse models were used, and our data confirmed the higher susceptibility of male mice to *T. cruzi* experimental infection than of female mice (25). The findings also demonstrated that DB2186 was the most promising candidate for *T. cruzi* infection as well as for *T. brucei* infection in murine models. It is important to consider that DB2186 exhibited consistently high selectivity indices for *T. cruzi* (123 and 640 for bloodstream trypano-

TABLE 6 Antitrypanosomal activities of quinolines in a mouse model of *T. b. rhodesiense* STIB900 infection

Compound	% parasite reduction after treatment with 3 doses of 40 mg/kg i.p.		No. of mice cured with 4 doses of 50 mg/kg i.p./no. of mice tested ^b
	1 day	3 days	
Pentamidine ^a	100 100	100 100	4/4 ^a
DB2104	>98 >98	>98 >98	NT
DB2131	>98 98	100 >98	0/4
DB2161	>98 >98	100 >98	0/4
DB2171	>98 >98	99 >98	0/4
DB2186	100 100	>98 >98	2/4
DB2187	>98 98	100 >98	0/4
DB2191	>98 >98	>98 >98	NT
DB2192	>98 >98	>98 >98	NT
DB2212	>98 >98	>98 >98	NT
DB2217	>98 >98	>98 100	4/4

^aPentamidine was tested at 3 doses of 4 mg/kg i.p. and at 4 doses of 1 mg/kg i.p. and cured all infected mice.

^bNT, not tested.

mastigote [BT] and intracellular forms) and *T. brucei* (1,761 for BT). It is interesting to note that DB2171 is much less active than two close analogues, DB2186 and DB2192, pointing to the importance of the urea fragment for activity compared to the simple amide unit.

The limited water solubility of the quinolines may have impaired a more successful *in vivo* result, which also was not improved by the use of other vehicles, including cyclodextrin and carboxymethylcellulose (data not shown). It is possible that minor structural modifications can improve their solubility, allowing further animal studies. The present set of results provides a basis for the development of novel quinoline derivatives, following medicinal chemistry approaches, presenting better solubility and improved potency, thus contributing to the identification of more effective and safe medicines to treat neglected tropical diseases such as Chagas disease and HAT.

MATERIALS AND METHODS

Compounds. The synthesis and characterization of the 10 quinolines (Table 1) can be found in the supplemental material. For *T. cruzi* assays, Bz (2-nitroimidazole; Laboratório Farmacêutico do Estado de Pernambuco [LAFEPE], Brazil) was used as a reference drug, and stock solutions were prepared in dimethyl sulfoxide (DMSO), with the final concentrations of the solvent never exceeding 0.6% and 10% in assays *in vitro* and *in vivo*, respectively, which are not toxic to the parasite, mammalian cells, and mice. For *T. b. rhodesiense*, pentamidine and melarsoprol were used as reference drugs. Pentamidine (Sigma) was dissolved in DMSO, and melarsoprol (Arsobal; Aventis) was dissolved in water.

Computational assessment of drug-like properties. Absorption, distribution, metabolism, excretion, and toxicity (ADMET and Lipinski's rule of five) properties of the studied quinolines were evaluated by using the PKCSM approach, which uses graph-based signatures to develop predictive ADMET (22, 24).

Parasites. (i) *T. cruzi*. BT forms of the Y strain were obtained from blood samples of infected albino Swiss mice at the peak of parasitemia. The purified parasites were resuspended in Dulbecco's modified Eagle medium (DMEM) supplemented with 10% fetal bovine serum as reported previously (25, 26). Trypomastigotes of the Tulahuen strain expressing the *Escherichia coli* β -galactosidase gene were collected from the supernatant of *T. cruzi*-infected L929 cultures as reported previously (16, 27).

(ii) *T. brucei*. *T. b. rhodesiense* strain STIB900, a derivative of strain STIB704, was isolated from a patient in Ifakara, Tanzania, in 1982 (28). Bloodstream forms were used for *in vitro* screening as well as for the acute mouse infection model, which mimics the first stage of HAT.

Mammalian cell cultures. For toxicity assays on mammalian cells, primary cultures of cardiac cells (CC) obtained from mouse embryos were plated onto 96-well plates previously coated with 0.01% gelatin (25). L929 cell lineages were obtained as described previously by Romanha et al. (16). L6 cells (rat skeletal myoblast; ATCC CRL-1458) were maintained in RPMI 1640 medium supplemented with 2 mM L-glutamine, 5.95 g/liter HEPES, 2 g/liter NaHCO₃, and 10% fetal bovine serum at 37°C in a humidified atmosphere containing 5% CO₂ (29).

***In vitro* cytotoxicity tests.** CC were incubated for 24 h at 37°C with different concentrations of each compound (up to 400 μ M) diluted in DMEM; the morphology, cell density, and spontaneous contractility were then evaluated by light microscopy; and cellular viability was determined by the PrestoBlue test as reported previously (27). L929 cells were incubated for 96 h at 37°C with different concentrations of each compound (up to 96 μ M) diluted in RPMI, and cellular viability was determined by the alamarBlue test as reported previously (27). The results were expressed according to the manufacturer's instructions, and the LC₅₀ value, which corresponds to the concentration that reduces cellular viability by 50%, was determined. Cytotoxicity assays performed by using L6 cells were conducted with a 72-h compound exposure time as previously reported (29). The selectivity index (SI) was expressed as the ratio between the LC₅₀ values obtained on host or L6 cells and the EC₅₀ obtained for the parasites.

Trypanocidal activity. For *T. cruzi* assays, BT of the Y strain (DTU II) (30) (5×10^6 BT per ml) were incubated for 2 and 24 h at 37°C in RPMI in the presence or absence of serial dilutions of the compounds (up to 32 μ M). After compound incubation, the death rates of parasites were determined by light microscopy through the direct quantification of the number of live parasites by using a Neubauer chamber, and the EC₅₀ (the compound concentration that reduces the number of parasites by 50%) was calculated (22). For assaying intracellular forms of the Y strain (DTU II), the most promising compound was further evaluated with infection of primary cultures of CC (using a ratio of 10 BT to 1 host cell). After 24 h of parasite interaction, the cultures were rinsed and incubated with the compounds for 48 h. After fixation with Bouin solution and staining with Giemsa solution, the percentage of CC infection and the mean number of parasites per infected cell were calculated by light microscopy for the determination of EC₅₀s of the infection index (II) (II = % infected host cells \times mean number of parasites per cell) (26). Culture-derived trypomastigotes of *T. cruzi* (Tulahuen strain expressing β -galactosidase [DTU VI]) were used to infect L929 cultures at a ratio of 10:1 (parasites/host cell). After 2 h, the cultures were washed and cultivated for another 48 h for the establishment of infection. The compounds were then added at increasing nontoxic concentrations to mammalian host cells, followed by maintenance at 37°C for 96 h for the determination of EC₅₀s. After the addition of 50 μ l of the substrate (CPRG [chlorophenol red glycoside] at 500 mM) in 0.5% Nonidet P40 and incubation at 37°C for 18 h, the absorbance at 570 nm was measured, and results were expressed as percent inhibition of the infection rate (16). For *T. brucei* assays, bloodstream forms of *T. b. rhodesiense* strain STIB900 were incubated in minimum essential medium (MEM) for 72 h in the presence of 3-fold serial dilutions at 37°C in a humidified atmosphere containing 5% CO₂. Parasite viability was assessed with the viability marker resazurin after a 3-day drug exposure time as previously reported (29).

Mouse acute toxicity. In order to determine the no-observed-adverse-effect level (NOAEL), increasing doses of the tested compounds (up to 200 mg/kg of body weight) were injected by the i.p. route individually into female Swiss mice (21 to 23 g; $n = 2$ per assay of the tested compounds). Treated animals were inspected for toxic and subtoxic symptoms according to Organization for Economic Cooperation and Development (OECD) guidelines (33). Forty-eight hours after compound injection, the NOAEL values were determined as reported previously (31). Biochemical analyses performed 48 h after compound exposure were performed at the ICTB platform (Fiocruz/RJ) as reported previously (17, 31).

Mouse infection and treatment. For acute *T. cruzi* infection models, male and female Swiss Webster mice (18 to 20 g) obtained from the animal facilities of ICTB were housed at a maximum of 7 per cage, kept in a specific-pathogen-free (SPF) room at 20°C to 24°C under a 12-h-light/12-h-dark cycle, and provided with sterilized water and chow *ad libitum*. The animals were allowed to acclimate for 7 days before the start of the experiments. Infection was performed by i.p. injection of 10^4 bloodstream trypomastigotes (Y strain). Age-matched noninfected mice were maintained under identical conditions (26). Quinolines were first dissolved in DMSO and then freshly diluted with sterile distilled water. The stock solution of Bz was prepared in sterile distilled water with 3% Tween 80 (Sigma-Aldrich). The animals were divided into the following groups ($n > 3$ per group): uninfected (noninfected and nontreated), untreated (infected but treated with the vehicle only), and treated (infected and treated with the compounds). Therapy was performed through the administration of 5 to 20 mg/kg at parasitemia onset (5 dpi) and the peak of parasitemia (8 dpi) according to an animal model reported previously (23). Alternatively, the most promising quinoline derivatives were administered for five consecutive days, starting at 5 dpi, using up to 25 mg/kg/day (i.p.) and 100 mg/kg/day Bz (orally [p.o.]). For all assays, only

mice with positive parasitemia were used in the infected groups. Parasitemia levels in *T. cruzi* assays were individually checked by direct microscopic counting of parasites in 5 μ l of blood, and mortality rates were checked daily until 30 days posttreatment and expressed as a percentage of cumulative mortality (CM) as described previously (27).

For *T. brucei* models, efficacy experiments were performed as previously reported (32), with modifications to soften the stringency of the mouse model of infection, and in line with the 3R principles for animal testing (reduce, refine, and replace), the number of mice was reduced in the primary *in vivo* screen. Female NMRI mice were infected i.p. with 10^4 *T. b. rhodesiense* STIB900 bloodstream trypanosomes. Experimental groups of two mice were treated with the new test compounds at 40 mg/kg i.p. on three consecutive days from day 1 to day 3 postinfection (total dose of 120 mg/kg i.p.). A control group was infected but remained untreated. The tail blood of all mice was checked microscopically for parasitemia reduction 24 h and 96 h after the last dose. Parasite reduction in mice treated with the experimental compounds was compared with that in the untreated control mice. Mice were euthanized at 96 h posttreatment if parasites were still detected in the tail blood. Aparasitemic mice were further examined twice per week for 30 days, or mice were euthanized after parasitemia relapses were detected. Mice that remained aparasitemic until day 30 were considered cured. The data from the follow-up efficacy study for compounds that achieved a parasite reduction of at least 98% in one of the two treated mice were comparable to those of groups of 4 infected mice treated for four consecutive days with a higher dosage of 50 mg/kg i.p. (total dose of 200 mg/kg i.p.). Pentamidine was used as a positive drug control, and it cured mice at 3×4 mg/kg and 4×1 mg/kg i.p.

Statistical analyses. Statistical analyses were performed by analysis of variance (ANOVA) with the level of significance set at a *P* value of ≤ 0.05 .

Ethics. All animal procedures performed at Fiocruz were carried out in accordance with the guidelines established by the Committee of Ethics for the Use of Animals (CEUA LW16/14). All protocols and procedures using animal models of *T. brucei* infection were reviewed and approved by the local veterinary authorities of the Canton Basel-Stadt, Switzerland.

SUPPLEMENTAL MATERIAL

Supplemental material for this article may be found at <https://doi.org/10.1128/AAC.01936-17>.

SUPPLEMENTAL FILE 1, PDF file, 0.4 MB.

ACKNOWLEDGMENTS

The present study was supported by grants from the Fundação Carlos Chagas Filho de Amparo a Pesquisa do Estado do Rio de Janeiro (FAPERJ), the Conselho Nacional de Desenvolvimento Científico e Tecnológico (CNPq), the Fundação Oswaldo Cruz, PDTIS, PAEF/CNPq/Fiocruz, and CAPES. M.N.C.S. is a research fellow of the CNPq and CNE Research. This work was also supported, in part, by National Institutes of Health grant no. AI06420 and by The Bill and Melinda Gates Foundation through a subcontract with the CPDD (to D.W.B. and R.B.).

We thank the Program for Technological Development in Tools for Health-PDTIS-FIOCRUZ for use of its facilities.

REFERENCES

- World Health Organization. 2017. Working to overcome the global impact of neglected tropical diseases: first WHO report on neglected tropical diseases. World Health Organization, Geneva, Switzerland. http://www.who.int/neglected_diseases/2010report/en/.
- Mackey TK, Liang BA, Cuomo R, Hafen R, Brouwer KC, Lee DE. 2014. Emerging and reemerging neglected tropical diseases: a review of key characteristics, risk factors and the policy and innovation environment. *Clin Microbiol Rev* 4:949–979. <https://doi.org/10.1128/CMR.00045-14>.
- Büscher P, Cecchi G, Jamonneau V, Priotto G. 2017. Human African trypanosomiasis. *Lancet* 390:2397–2409. [https://doi.org/10.1016/S0140-6736\(17\)31510-6](https://doi.org/10.1016/S0140-6736(17)31510-6).
- Chatelain E. 2015. Chagas disease drug discovery: toward a new era. *J Biomol Screen* 1:22–35. <https://doi.org/10.1177/1087057114550585>.
- Chatelain E, Konar N. 2015. Translational challenges of animal models in Chagas disease drug development: a review. *Drug Des Devel Ther* 9:4807–4823. <https://doi.org/10.2147/DDDT.S90208>.
- Molina I, Salvador F, Sánchez-Montalvá A. 2015. The use of posaconazole against Chagas disease. *Curr Opin Infect Dis* 5:397–407. <https://doi.org/10.1097/QCO.0000000000000192>.
- Morillo CA, Marin-Neto JA, Avezum A, Sosa-Estani S, Rassi A, Jr, Rosas F, Villena E, Quiroz R, Bonilla R, Britto C, Guh LF, Velazquez E, Bonilla L, Meeks B, Rao-Melacini P, Pogue J, Mattos A, Lazdins J, Rassi A, Connolly SJ, Yusuf S, BENEFIT Investigators. 2015. Randomized trial of benznidazole for chronic Chagas' cardiomyopathy. *N Engl J Med* 14:1295–1306. <https://doi.org/10.1056/NEJMoa1507574>.
- Devine W, Thomas SM, Erath J, Bachovchin KA, Lee PJ, Leed SE, Rodriguez A, Sciotti RJ, Mensa-Wilmot K, Pollastri MP. 2017. Antiparasitic lead discovery: toward optimization of a chemotype with activity against multiple protozoan parasites. *ACS Med Chem Lett* 3:350–354. <https://doi.org/10.1021/acsmchemlett.7b00011>.
- Chatelain E. 2017. Chagas disease research and development: is there light at the end of the tunnel? *Comput Struct Biotechnol J* 15:98–103. <https://doi.org/10.1016/j.csbj.2016.12.002>.
- Don R, Ioset JR. 2013. Screening strategies to identify new chemical diversity for drug development to treat kinetoplastid infections. *Parasitology* 141:140–146. <https://doi.org/10.1017/S003118201300142X>.
- Field MC, Horn D, Fairlamb AH, Ferguson MA, Gray DW, Read KD, De Rycker M, Torrie LS, Wyatt PG, Wyllie S, Gilbert IH. 2017. Anti-trypanosomatid drug discovery: an ongoing challenge and a continuing need. *Nat Rev Microbiol* 4:217–231. <https://doi.org/10.1038/nrmicro.2016.193>.
- Keenan M, Chaplin JH. 2015. A new era for Chagas disease drug discov-

- ery? *Prog Med Chem* 54:185–230. <https://doi.org/10.1016/bs.pmch.2014.12.001>.
13. Bahia MT, Nascimento AF, Mazzeti AL, Marques LF, Gonçalves KR, Mota LW, Diniz LDF, Caldas IS, Talvani A, Shackelford DM, Koltun M, Saunders J, White KL, Scandale I, Charman SA, Chatelain E. 2014. Antitrypanosomal activity of fexinidazole metabolites, potential new drug candidates for Chagas disease. *Antimicrob Agents Chemother* 58:4362–4370. <https://doi.org/10.1128/AAC.02754-13>.
 14. Tatipaka HB, Gillespie JR, Chatterjee AK, Norcross NR, Hulverson MA, Ranade RM, Nagendar P, Creason SA, McQueen J, Duster NA, Nagle A, Supek F, Molteni V, Wenzler T, Brun R, Glynne R, Buckner FS, Gelb MH. 2014. Substituted 2-phenylimidazopyridines: a new class of drug leads for human African trypanosomiasis. *J Med Chem* 57:828–835. <https://doi.org/10.1021/jm401178t>.
 15. Patrick DA, Wenzler T, Yang S, Weiser PT, Wang MZ, Brun R, Tidwell RR. 2016. Synthesis of novel amide and urea derivatives of thiazol-2-ethylamines and their activity against *Trypanosoma brucei rhodesiense*. *Bioorg Med Chem* 24:2451–2465. <https://doi.org/10.1016/j.bmc.2016.04.006>.
 16. Romanha AJ, de Castro SL, Soeiro MNC, Lannes-Vieira J, Ribeiro I, Talvani A, Bourdin B, Blum B, Olivieri B, Zani C, Spadafora C, Chiari E, Chatelain E, Chaves G, Calzada JE, Bustamante JM, Freitas LH, Jr, Romero LI, Bahia MT, Lotrowska M, Soares M, Andrade SG, Armstrong T, Degrave W, Andrade ZA. 2010. *In vitro* and *in vivo* experimental models for drug screening and development for Chagas disease. *Mem Inst Oswaldo Cruz* 105:233–238. <https://doi.org/10.1590/S0074-02762010000200022>.
 17. Soeiro MNC, Werbovets K, Boykin DW, Wilson WD, Wang MZ, Hemphill A. 2013. Novel amidines and analogues as promising agents against intracellular parasites: a systematic review. *Parasitology* 140:929–951. <https://doi.org/10.1017/S0031182013000292>.
 18. Peña I, Pilar Manzano M, Cantizani J, Kessler A, Alonso-Padilla J, Bardera Al, Alvarez E, Colmenarejo G, Cotillo I, Roquero I, de Dios-Anton F, Barroso V, Rodriguez A, Gray DW, Navarro M, Kumar V, Sherstnev A, Drewry DH, Brown JR, Fiandor JM, Julio Martin J. 2015. New compound sets identified from high throughput phenotypic screening against three kinetoplastid parasites: an open resource. *Sci Rep* 5:8771. <https://doi.org/10.1038/srep08771>.
 19. Williams K, Bilsland E, Sparkes A, Aubrey W, Young M, Soldatova LN, De Grave K, Ramon J, de Clare M, Sirawaraporn W, Oliver SG, King RD. 2015. Cheaper faster drug development validated by the repositioning of drugs against neglected tropical diseases. *J R Soc Interface* 104:20141289. <https://doi.org/10.1098/rsif.2014.1289>.
 20. Katsuno K, Burrows JN, Duncan K, Hoof van Huijsduijnen R, Kaneko T, Kita K, Mowbray CE, Schmatz D, Warner P, Slingsby BT. 2015. Hit and lead criteria in drug discovery for infectious diseases of the developing world. *Nat Rev Drug Discov* 11:751–758. <https://doi.org/10.1038/nrd4683>.
 21. Rassi A, Jr, Marin Neto JA, Rassi A. 2017. Chronic Chagas cardiomyopathy: a review of the main pathogenic mechanisms and the efficacy of aetiological treatment following the BENznidazole Evaluation for Interrupting Trypanosomiasis (BENEFIT) trial. *Mem Inst Oswaldo Cruz* 3:224–235. <https://doi.org/10.1590/0074-02760160334>.
 22. Nefertiti ASG, Batista MM, Da Silva PB, Torres-Santos EC, Cunha EF, Jr, Green J, Kumar A, Farahat AA, Boykin DW, Soeiro MNC. 2017. Antiparasitic effect of novel amidines against *Trypanosoma cruzi*: phenotypic and *in silico* absorption, distribution, metabolism, excretion and toxicity analysis. *Parasitol Open* 5:e5. <https://doi.org/10.1017/pao.2017.5>.
 23. Guedes-da-Silva FH, Batista DG, da Silva CF, Meuser MB, Simões-Silva MR, de Araújo JS, Ferreira CG, Moreira OC, Britto C, Lepesheva GI, Soeiro MDN. 2015. Different therapeutic outcomes of benznidazole and VNI treatments in different genders in mouse experimental models of *Trypanosoma cruzi* infection. *Antimicrob Agents Chemother* 12:7564–7570. <https://doi.org/10.1128/AAC.01294-15>.
 24. Pires DE, Blundell TL, Ascher DB. 2015. pkCSM: predicting small-molecule pharmacokinetic and toxicity properties using graph-based signatures. *J Med Chem* 9:4066–4072. <https://doi.org/10.1021/acs.jmedchem.5b00104>.
 25. Meirelles MN, De Araujo-Jorge TC, Miranda CF, De Souza W, Barbosa HS. 1986. Interaction of *Trypanosoma cruzi* with heart muscle cells: ultrastructural and cytochemical analysis of endocytic vacuole formation and effect upon myogenesis *in vitro*. *Eur J Cell Biol* 41:198–206.
 26. Batista DG, Pacheco MG, Kumar A, Branowska D, Ismail MA, Hu L, Boykin DW, Soeiro MN. 2010. Biological, ultrastructural effect and subcellular localization of aromatic diamidines in *Trypanosoma cruzi*. *Parasitology* 2:251–259. <https://doi.org/10.1017/S0031182009991223>.
 27. Timm BL, da Silva PB, Batista MM, da Silva FHG, da Silva CF, Tidwell RR, Patrick DA, Jones SK, Bakunov SA, Bakunova SM, Soeiro MNC. 2014. *In vitro* and *in vivo* biological effect of novel arylimidamide derivatives against *Trypanosoma cruzi*. *Antimicrob Agents Chemother* 7:3720–3726. <https://doi.org/10.1128/AAC.02353-14>.
 28. Brun R, Schumacher R, Schmid C, Kunz C, Burri C. 2001. The phenomenon of treatment failures in human African trypanosomiasis. *Trop Med Int Health* 6:906–914. <https://doi.org/10.1046/j.1365-3156.2001.00775.x>.
 29. Bakunov SA, Bakunova SM, Wenzler T, Ghebru M, Werbovets KA, Brun R, Tidwell RR. 2010. Synthesis and antiprotozoal activity of cationic 1,4-diphenyl-1-H-1,2,3-triazoles. *J Med Chem* 53:254–272. <https://doi.org/10.1021/jm901178d>.
 30. Zingales B, Andrade SG, Briones MR, Campbell DA, Chiari E, Fernandes O, Guhl F, Lages-Silva E, Macedo AM, Machado CR, Miles MA, Romanha AJ, Sturm NR, Tibayrenc M, Schijman AG. 2009. A new consensus for *Trypanosoma cruzi* intraspecific nomenclature: second revision meeting recommends TcI to TcVI. *Mem Inst Oswaldo Cruz* 7:1051–1054. <https://doi.org/10.1590/S0074-02762009000700021>.
 31. Da Silva CF, Batista DDG, Oliveira GM, de Souza EM, Hammer ER, da Silva PB, Daliry A, Araujo JS, Britto C, Rodrigues AC, Liu Z, Farahat AA, Kumar A, Boykin DW, Soeiro MDNC. 2012. *In vitro* and *in vivo* investigation of the efficacy of arylimidamide DB1831 and its mesylated salt form—DB1965—against *Trypanosoma cruzi* infection. *PLoS One* 1:e30356. <https://doi.org/10.1371/journal.pone.0030356>.
 32. Wenzler T, Yang S, Patrick DA, Braissant O, Ismail MA, Tidwell RR, Boykin DW, Wang MZ, Brun R. 2014. *In vitro* and *in vivo* evaluation of 28DAP010, a novel diamidine for treatment of second-stage African sleeping sickness. *Antimicrob Agents Chemother* 8:4452–4463. <https://doi.org/10.1128/AAC.02309-13>.
 33. Organisation for Economic Co-operation and Development. 2017. OECD guidelines for the testing of chemicals. OECD, Paris, France. <http://www.oecd.org/chemicalsafety/testing/oecdguidelinesforthetestingofchemicals.htm>.